Bioresource Technology Reports 24 (2023) 101673

Contents lists available at ScienceDirect

Bioresource Technology Reports

journal homepage: www.sciencedirect.com/journal/bioresource-technology-reports

# Comparative techno-economic assessment of production of microcrystalline cellulose, microcrystalline nitrocellulose, and solid biofuel for biorefinery of pistachio shell

Alireza Chackoshian Khorasani *, Saeed Zeinabadi Bajestani, Alireza Saadat Bajestani

*Department of Chemical Engineering, Faculty of Engineering, Ferdowsi University of Mashhad, Mashhad, Iran*

ARTICLE INFO

*Keywords:*
Pistachio shell
Microcrystalline cellulose
Nitrocellulose
Biochar
Biofuel
Biorefinery

ABSTRACT

The biorefinery of pistachio shell (PS) for producing microcrystalline cellulose (MC), microcrystalline nitrocellulose (MNC), and biochar (PSB) was techno-economically assessed. A rapid recyclable nitric acid treatment purely isolated 32–41 % of PS as MC particles (crystallinity index of 86 %) at 80 °C for 90 min. A facile synthesis obtained MNC particles (crystallinity index of 79 %) with a nitrogen content of 10.81 % from the MC. The PSB with the HHV value of 27.82 MJ/kg and 24 % production yield was achieved as biocoal via pyrolysis at 400 °C for 30 min. The incorporation of sulfuric acid pre-dehydration with pyrolysis temperature and time improved the PSB yield up to 28 %, while lowering the HHV to 24.12 MJ/kg. The NPV, IRR, ROI, and payback time indicated that the MC and MNC production from PS could make them suitable for future commercialization; however, the PSB production was not profitable because it could not compete with coal.

## 1. Introduction

One of the most critical environmental concerns is the increase in agricultural waste that can be biorefined to valuable products. The agricultural residues, such as lignocellulosic biomass, are comprised of cellulose, hemicellulose, and lignin (Kasiri and Fathi, 2018).

Cellulose is the most abundant biopolymer in the world, which consists of glucose monomers linked together via β-1,4 bonds. Its approximate annual production is estimated $10^{10}$–$10^{12}$ tons. It is obtained from plant sources such as wood, cotton, linen, jute, sugarcane bagasse, and cereal straw, as well as from microbial fermentation (Kasiri and Fathi, 2018; Movva and Kommineni, 2017). One of the major agricultural products in Iran is pistachio. Iran is addressed as the largest pistachio producer in the world. Around 45 % of the pistachio is its shell (PS), mostly used for livestock and charcoal feedstock (Kasiri and Fathi, 2018; Robles et al., 2021). However, PS has a high capability to be converted into cellulose because around 50 % of it is cellulose. Few studies reported the cellulose production from PS. Cellulose nanocrystals (CNC) were isolated using alkaline pretreatment and sulfuric acid-based hydrolysis (Kasiri and Fathi, 2018; Marett et al., 2017; Movva and Kommineni, 2017). Cellulose nanofibers (CNF) were extracted from PS using alkaline pretreatment for nanopaper making (Robles et al., 2021). Furthermore, microwave-assisted alkali pretreatment (Özbek et al., 2021), ultrasound-assisted alkali pretreatment, and sequential ultrasound-microwave-assisted alkaline pretreatment (Özbek et al., 2020) were investigated for the fractionation of cellulose from PS. Cellulose consists of crystalline and amorphous phases. The latter is easily hydrolyzed by strong acid hydrolysis. These hydrolyzed materials are called microcrystalline cellulose. It has received much attention and interest in academic and industrial fields due to its excellent properties (Trache et al., 2014). However, its isolation from PS was not reported.

Nitrocellulose (NC) has a cellulose structure in which the hydroxyl groups of carbons 2, 3, and 6 are replaced by nitro groups. It consists of crystalline and amorphous regions. Microcrystalline nitrocellulose (MNC) is considered a precious material and a good fuel because the reduction of its amorphous regions and the improvement of its crystallinity effectively reduce its sensitivity (Meng et al., 2020). NC, the most prominent industrial cellulose ester, has different properties and applications (Muvhiiwa et al., 2021). With a small percentage of nitrogen (below 12 %), it is used in coatings, microelectronics, membranes, biosensors, and printing. With a high percentage of nitrogen (above 12 %), it is used as solid fuel, explosives, fireworks, and gas generators due to its high energy (Tarchoun et al., 2019; Trache et al., 2016). The most common feedstocks for NC are wood and cotton. Due to their other

* Corresponding author at: Department of Chemical Engineering, Faculty of Engineering, Ferdowsi University of Mashhad, P.O. Box 91779-48974, Mashhad, Iran.
*E-mail address:* chakoshian@um.ac.ir (A.C. Khorasani).

https://doi.org/10.1016/j.biteb.2023.101673
Received 14 September 2023; Received in revised form 12 October 2023; Accepted 21 October 2023
Available online 24 October 2023

applications, other feedstocks should be explored for NC production (Tarchoun et al., 2019). For MNC production, various feedstocks, such as alpha-grass fibers (Trache et al., 2016) and *Posidonia oceanica* (Tarchoun et al., 2019), were studied. Further, its production from purchased analytical-grade MC was reported (Meng et al., 2020; Santos et al., 2021).

Considering the importance of energy and the environmental challenges of the consumption of non-renewable energy, the utilization of agricultural waste to produce renewable energy is one of the most important environmentally friendly approaches. Rare attempts were made in the feasibility study of biofuel production from PS. The kinetics and mechanism of its thermal degradation during the pyrolysis were investigated for efficient design and optimization of thermochemical processes for bioenergy generation (Açıkalın, 2012; Gupta et al., 2022; Peters, 2011). Further, PS biochar, pyrolyzed at 550 °C, was addressed as solid fuel by another study (Jeníček et al., 2023). However, the primary concern of these studies was not to increase the production yield of solid biofuel and its HHV.

According to the literature, several studies were conducted on the extraction of cellulose from PS, but MC has not been achieved. Further, few research were carried out in the production of MNC from various raw materials, but PS has not been investigated as feedstock. Further, the kinetics and mechanism of biofuel production from PS via pyrolysis were studied, but acid pre-dehydration incorporating with pyrolysis temperature and time has not been investigated for improving the HHV and production yield of solid biofuel from PS (PSB). Moreover, the cost analysis of production of MC, MNC, and PSB from PS has not been assessed. Therefore, a comparative techno-economic assessment can be conducted on the feasibility of production of MC, MNC, and PSB for valorization of PS. For these objectives, this study contributed to the MC extraction from PS by recyclable nitric acid treatment, the MNC synthesis from MC, and the PSB production from PS via pyrolysis (Scheme 1). The samples were characterized using SEM, FTIR, XRD, TG, and CHNSO analyses. Finally, the economic evaluation of MC, MNC, and PSB was carried out.

## 2. Materials and methods

### 2.1. Materials

PS were collected from the pistachio available in the local market of Mashhad (Iran) and chopped to sizes <5 mm. All chemicals (analytical grade) were purchased from Dr. Mojallali (Tehran, Iran) and used as received without further purification.

### 2.2. Isolation of microcrystalline cellulose

PS were subjected to the acid treatment. For acid treatment, 10 g of PS were added to 100 mL of $HNO_3$ (3 mol/L) aqueous solution and kept at 80 °C for 90 min (this experiment was also assessed for 30 and 60 min). Afterwards, the precipitated solid was added to NaClO aqueous solution (2.5 wt%) and kept at room temperature for 30 min. The obtained solid residue was washed up several times using deionized water, and then dried as MC. The acid solution, drained after the treatment, was recycled and reused for the acid treatment, repeated four cycles.

The determination of cellulose content and cellulose isolation yield was carried out with following procedure: In order to remove all the lignin and main part of pentosans based on Kürschner's method, the

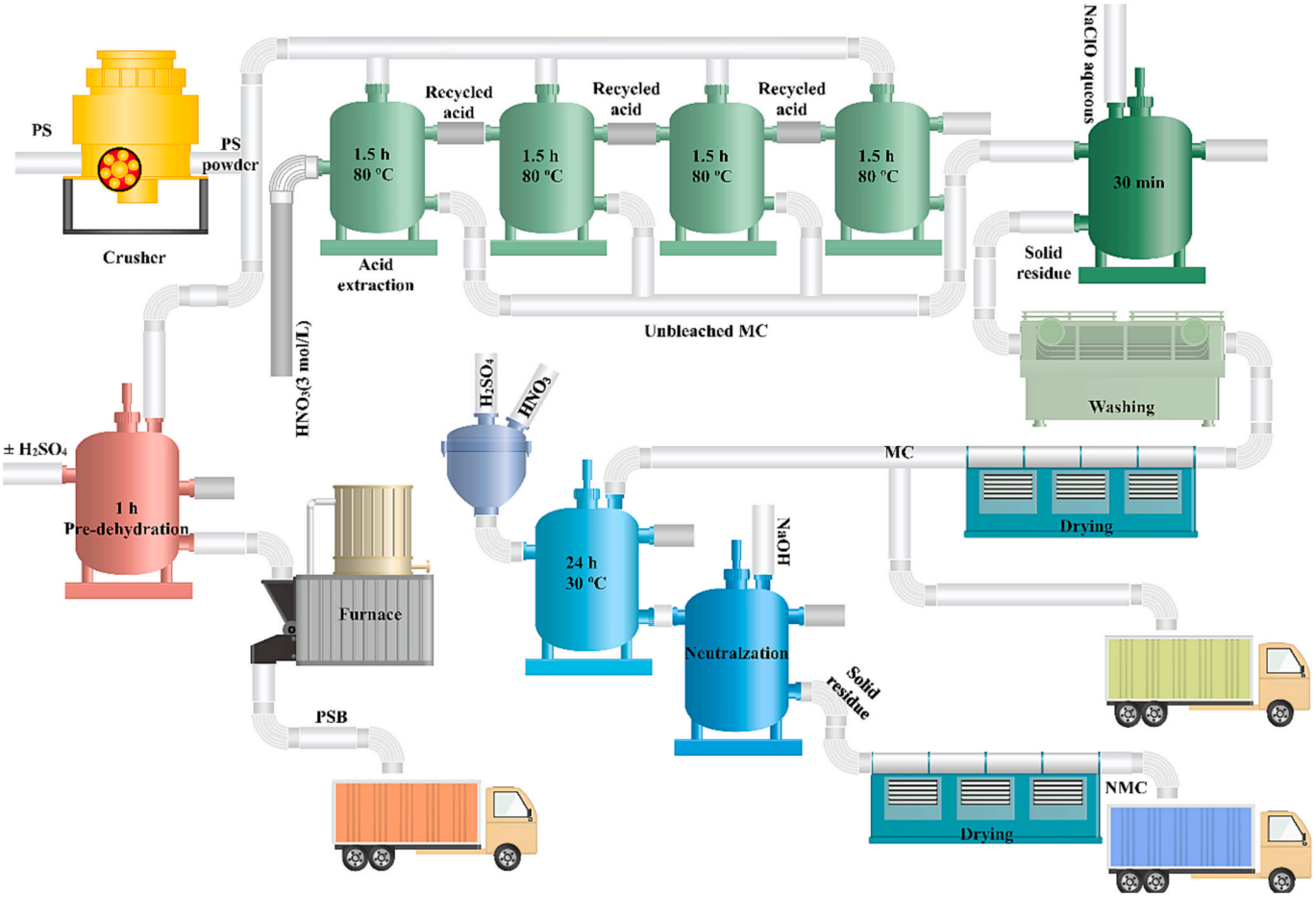


**Scheme 1.** Schematic illustration for the production of MC, NMC, and PSB from PS.

sample (1 g) was treated with 25 mL of the mixture of ethanol: nitric acid in a ratio of 4:1 (v/v) under reflux for 1 h. After the treatment, the solid residue was filtered, washed with deionized water, and dried (Paloheimo and Kero, 1962). Then, the dried residue was treated with 100 mL of acid detergent solution (1 N $H_2SO_4$) under reflux for 1 h. After that, the solid product was filtered, washed with deionized water, and dried to obtain cellulose (Pattnaik et al., 2022). The cellulose content was calculated using Eq. (1):

$$\text{Cellulose content } (\%) = \frac{cellulose\ mass}{sample\ mass} \times 100 \quad (1)$$

Also, the cellulose isolation yield was calculated using Eq. (2):

$$\text{Isolation yield } (\%) = \frac{cellulose\ mass}{PS\ mass} \times 100 \quad (2)$$

### 2.3. Preparation of microcrystalline nitrocellulose

The obtained MC were used as raw material for the preparation of MNC. 10 g of MC were added to 100 mL of $HNO_3$-$H_2SO_4$ aqueous solution ($HNO_3$:$H_2SO_4$ = 40:60) and kept at 30 °C for 24 h. Afterwards, the obtained solid residue was neutralized, washed up several times using deionized water, and then dried as MNC.

Nitrogen content of MNC was determined by elemental analysis of carbon, hydrogen, nitrogen, sulfur, and oxygen (CHNSO) with a Thermo Finnigan Flash EA 1112 device.

### 2.4. Preparation of solid biofuel

In order to prepare solid biofuel from PS, three factors of pyrolysis temperature, pyrolysis duration, and acid pre-dehydration were investigated. To pre-dehydrate PS, 1 g of PS was mixed with 1 mL (1.83 g) of $H_2SO_4$ (98 %) for 1 h. The obtained black solid residue was separated for further use as pre-dehydrated PS. The PS and pre-dehydrated PS were pyrolyzed at three temperatures of 200, 300, and 400 °C for 0 and 30 min retention time. The pyrolysis was carried out with a heating rate of 40 °C/min from the ambient temperature to the set temperature. When the furnace reached the set temperature, it was turned off, and cooled down for 2 h through heat exchange with the environment. Then, the pyrolyzed sample, called pistachio shell biochar (PSB), was evaluated.

The solid biofuel yield was calculated using Eq. (3):

$$Product\ yield\ (\%) = \frac{m_{PSB}}{m_{PS}} \times 100 \quad (3)$$

where, $m_{PSB}$ (g) and $m_{PS}$ (g) are the mass of PSB and PS, respectively.

Higher heating value (HHV) of solid biofuel was calculated from the ultimate analysis for elemental composition (CHNSO) of samples, carried out with a CHNS analyzer (Thermo Finnigan Flash EA 1112, Thermo Fischer Scientific, USA), by Dulong's equation as expressed in Eq. (4):

$$\text{HHV } (MJ/kg) = 0.3383C + 1.422\ (H–O/8) \quad (4)$$

The HHV yield (HY) of solid biofuel was calculated using Eq. (5):

$$HY\ (MJ/kg) = \frac{HHV \times Yield}{100} \quad (5)$$

Also, H/C and O/C atomic ratios were calculated using data from CHNSO.

### 2.5. Characterizations

#### 2.5.1. SEM analysis

The morphology and structure of samples were characterized using scanning electron microscopy (SEM) (XL30, Philips, Netherlands). For these analyses, the samples were dried, coated with gold using the sputtering technique, fractured, and observed at beam energy of 20.00 kV.

#### 2.5.2. FTIR analysis

The functional groups of samples were analyzed using FTIR spectrometer (Spectrum 100, Perkin Elmer, USA) with the anhydrous KBr pellet method. For each sample, the scanning region was recorded in the range of 400–4000 $cm^{-1}$.

#### 2.5.3. XRD analysis

The crystallinity of samples was determined using X-ray diffractometer (XRD) (X'Pert MPD, Philips, Netherlands) with Cu Kα radiation (λ = 0.1542 nm; 40 kV and 30 mA) in 2θ angle range of 10°–40° with the scan rate at 0.02°/s. The crystallinity index (CrI) of samples was estimated using Segal' method (Eq. (6)) based on the maximum intensity near $2\theta = 22.5°$ ($I_{200}$) and the minimum intensity around $2\theta = 18.5°$ ($I_{am}$) (Boufi and Chaker, 2016).

$$\text{CrI } (\%) = \frac{I_{200} - I_{am}}{I_{200}} \times 100 \quad (6)$$

#### 2.5.4. Thermal analysis

The thermal stability of samples was determined using TGA device (METTLER, SW14, United States). For each sample, it was heated from the room temperature to 600 °C at the rate of 10 °C/min under nitrogen gas with a flow rate of 100 mL/min.

### 2.6. Economic assessment

The techno-economic assessment of production of MC, MNC, and PSB was carried out. The total capital investment was estimated as the sum of the major equipment and installation costs, and indirect capital costs. The total annual operating cost was the sum of the materials, utilities, labor, supplies, fixing, and general works costs. For the estimation of revenue, MC, MNC, and PSB were assumed to be sold at 60, 2450, and 0.136 $/kg, respectively. The selling prices of MC and MNC were adopted from Merck (Germany), and PSB price was determined based on the annual average price of coal. The profitability analysis of the process simulation was performed with the selling price, unit production costs, net profit, net profit margin, return of investment (ROI), payback period, internal rate of return (IRR), net present value (NPV) through the cash flow analysis. They were calculated based on the operational time of 288 days, an income tax of 20 %, and an annual interest rate of 25 %. Cash flow analysis was used following straight-line depreciation method over a period of 15 years.

## 3. Results and discussion

### 3.1. MC production

The isolation yield and cellulose content for PS and MC in different acid treatment times are presented in Table 1. For the sample of PS, extracting the cellulose using the standard method results in pure cellulose with 48.50 ± 2.12 % isolation yield. The results show that the MC isolation yields are not statistically significant ($p > 0.05$). Considering the extraction time extended by the reduction of acid solution hydrolyzability after each cycle, the desired extraction time was determined as 90 min because the acid solution was intended to be reused (Fig. 1). The results revealed that reusing the acid solution successfully resulted in the

**Table 1**
Isolation yield and cellulose content for PS, and MC in various time.

| Sample | Isolation yield (%) | Cellulose content (%) |
|---|---|---|
| PS | 48.50 ± 2.12 | 100.00 |
| $MC_{30}$ | 39.60 ± 2.26 | 100.00 |
| $MC_{60}$ | 34.50 ± 2.12 | 100.00 |
| $MC_{90}$ | 33.50 ± 2.12 | 100.00 |

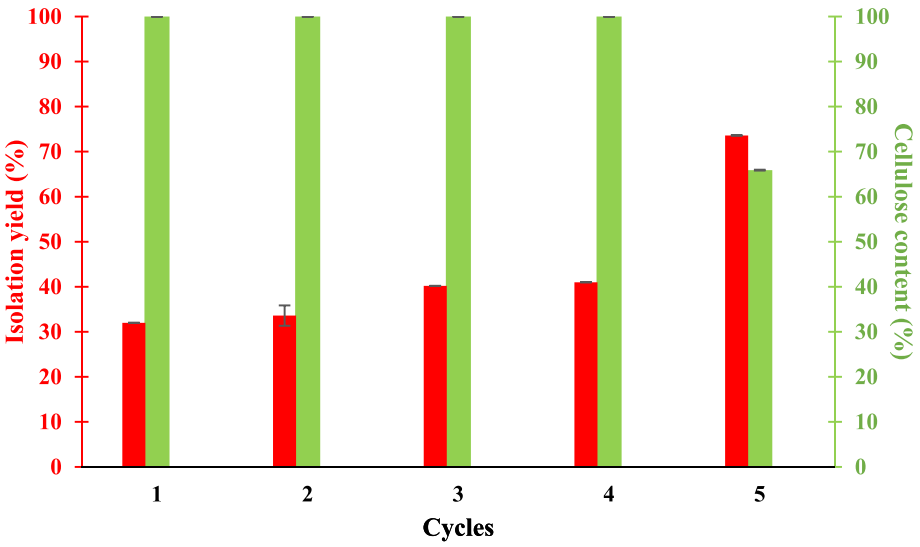


**Fig. 1.** The effect of recycled acid solution on the isolation yield and cellulose content for 90-min acid extraction.

production of pure MC with isolation yields in the range of 32–41 % for four cycles. In the acid extraction, water molecules ($H_2O$) and hydrogen ions ($H^+$) from nitric acid created hydrogen bonds with hydroxyl functional groups (OH) in hemicellulose and three monolignols (p-coumaryl, coniferyl, and sinapyl alcohols) in lignin, causing the structure of lignin-hemicellulose-cellulose was interconnected in PS. As a result, hemicellulose and lignin were separated from the PS structure and became soluble in the acid solution, remaining crystalline cellulose as solid product. This occurred in the first four cycles completely and resulted in the production of pure cellulose. On the other hand, each solvent has a limited capacity to dissolve a solute. Here, the acid solution could completely dissolve the PS impurities based on the defined process conditions such as temperature, solid-to-liquid ratio, and time in four cycles to produce pure cellulose with 100 % content. However, during the fifth cycle, the dissolving capacity of acid solution was limited and the solution became saturated with hemicellulose and lignin molecules extracted in the previous four cycles. Therefore, the product in cycle 5 was not pure cellulose and was composed of cellulose, hemicellulose and lignin molecules not extracted into the saturated acid solution. For this reason, the cellulose content of the product in cycle 5 decreased to 65.90 %.

Compared to other research, this work successfully demonstrated the isolation of MC from PS for the first time, although the CNC and CNF obtained from PS were reported in previous studies (Kasiri and Fathi, 2018; Marett et al., 2017; Robles et al., 2021). On the other hand, the main procedure of cellulose extraction was the alkaline treatment of PS during several steps (Kasiri and Fathi, 2018; Marett et al., 2017; Movva and Kommineni, 2017; Özbek et al., 2021, 2020; Robles et al., 2021), whereas MC was obtained using the nitric acid treatment in one pot. Nitric acid could remove the lignin from PS, and the ether bonds of hemicellulose could be broken to remove it. This resulted in the isolation of pure MC from PS (Wang et al., 2020). A lower isolated MC than the extractable cellulose of PS could be due to the amorphous regions of cellulose dissolved with nitric acid, while the crystalline regions were acid-resistant and remained (Cheng et al., 2020). In contrast, alkaline treatment resulted in approximately 90–100 % cellulose recovery, but the product was impure because the treatment could not remove all lignin and hemicellulose from PS (Özbek et al., 2021, 2020).

### 3.2. MNC production

The results showed that the weight of MNC increased by 25 % compared to MC due to the MC nitration leading to the addition of nitro groups to MC. As given in Table 2, the nitrogen content of MNC was found to be 10.81 %. The content of carbon and hydrogen decreased, and the oxygen increased because of the $NO_2$ groups. Other studies reported the nitrogen content of NC in the range of 10.64–12.56 % (Gismatulina et al., 2018; Lipin et al., 2020; Muvhiiwa et al., 2021; Saginovich et al., 2020; Tarchoun et al., 2019; Trache et al., 2016). This was due to the nitration process conditions such as used acids and their mixture, temperature, time, solid-to-liquid ratio, and type of rector. Compared to other studies, this work was proceeded under a more suitable and economical condition. In contrast, their methods were more expensive and complicated, such as the use of a supercritical static reactor and carbon dioxide medium (Saginovich et al., 2020). In addition, feedstocks investigated for cellulose isolation could be influential because they determined the cellulose character affecting the NC quality. Various raw materials, such as *Miscanthus* cellulose (Gismatulina et al., 2018), tobacco stalks (Muvhiiwa et al., 2021), cotton pulp (Saginovich et al., 2020), deciduous trees (Lipin et al., 2020), alpha-grass fibers (Trache et al., 2016), and *Posidonia oceanica* (Tarchoun et al., 2019), were studied to produce NC. However, few of them were conducted on the MNC production. PS was investigated in this research for the first time, while alpha-grass fibers (Trache et al., 2016) and *Posidonia oceanica* (Tarchoun et al., 2019) had resulted in MNC with a nitrogen content of 12.56 % and 12.55 %, respectively. Consequently, the resultant MNC can be utilized for coatings, microelectronics, biosensors, lacquers, inks, membranes, magnetic filtration, and adhesives due to its nitrogen content below 12 % (Tarchoun et al., 2019; Trache et al., 2016).

### 3.3. PSB production

In order to find the desirable condition for producing solid biofuel from PS, the effect of interactions of pyrolysis temperature and time, and acid pre-dehydration was studied on the properties of 12 PSBs prepared

**Table 2**
Ultimate analysis of CHNSO for MC and MNC.

| Sample | Ultimate analysis (wt%) | | | | | |
|---|---|---|---|---|---|---|
| | C | H | N | S | O[a] | Ash |
| MC | 40.86 ± 0.40 | 6.13 ± 0.10 | 0.43 ± 0.00 | 0 | 52.58 ± 0.42 | 0 |
| MNC | 26.33 ± 0.24 | 2.89 ± 0.04 | 10.81 ± 0.00 | 0 | 59.97 ± 0.44 | 0 |

[a] O (%) = 100-C (%)-H (%)-N (%)-ash (%).

as conditions given in Table 3.

The results demonstrated that the pre-dehydration provided PSBs with higher yields (T ≥ 300 °C) and lower HHVs. The pre-dehydration of biomass improved the product yield during pyrolysis by changing the structure of cellulose and hemicellulose into polycyclic aromatic layers of carbon because carbohydrates could be carbonized using concentrated sulfuric acid (≥96 wt%). It rapidly removed O and H elements via its strong dehydration with the formation of $H_2O$ and release of heat (Wang et al., 2022). As shown in Fig. 2, the pre-dehydration distances the pre-dehydrated PSBs from the coal region. Moreover, it sulfurized the pre-dehydrated PSBs, which was inevitable at low pyrolysis temperatures and short pyrolysis time. However, their sulfur was removed as sulfur dioxide ($SO_2$) with increasing temperature and time (Table 3). This gas contaminated air that should be recycled to produce sulfuric acid.

Pyrolysis temperature and time are the most crucial process parameters affecting the yield, HHV, and ultimate analysis of the product. The results revealed that the rise in the pyrolysis temperature and time increased PSB carbon content, leading to its higher HHV and its lower yield (Table 3). As shown in Fig. 2, increasing the temperature and time drives the location of PSBs close to the coal region due to the removal of hydroxyl groups (—OH), carboxyl groups (—COOH), and carbonyl (—CO—) from the structure of PS (Barskov et al., 2019), modifying the coal properties of PSBs.

The yield, HHV, and coal properties of a product play a critical role in its qualification as a solid fuel. According to the different data for the yield and HHV of PSBs (Table 3), the HY and coal properties helped to select the desirable solid biofuel. Therefore, PSB 12 with the HHV of 27.82 MJ/kg and yield of 24 % was selected. It was achieved without pre-dehydration and with pyrolysis at 400 °C for 30 min. It was the only PSB in the coal region, whereas its HY was not higher than that of other PSBs (Fig. 2).

According to the literature, only one study addressed PS biochar as fuel in which only the pyrolysis temperature was investigated as a process parameter (Jeníček et al., 2023). It showed that the biochar, pyrolyzed at 350 °C for 30 min, was similar to PSB 12 in terms of HHV (Table 4). As the research conducted on improving the biochar yield of Douglas fir sawdust, sulfuric acid pre-dehydration enhanced its yield from 22.4 to 44 %, reduced its HHV from 32.18 to 31.16 MJ/kg, and diminished the coal properties (Wang et al., 2022), which agreed with this study. It presented only the effect of pre-dehydration on the resulting biochar (Wang et al., 2022). Thus, this study, for the first time, demonstrated in a more profound way the simultaneous influence of $H_2SO_4$ pre-dehydration, the pyrolysis temperature and time on PSB yield, its HHV, and its coal properties.

### 3.4. Characterizations

#### 3.4.1. Surface morphology

The surface morphology of PS, MC, MNC, and PSB is depicted in Fig. S1. The SEM of PS demonstrates the homogeneous particles with the macropores surfaces (Fig. S1A). They are irregular in shape and not uniform in size. Their dimensions are varied in the range of 100–600 μm. Compared to MC, MNC, and PSB, PS particle sizes are very different from each other.

As shown in Fig. S1B and C, the shape and size of the particles of MC and MNC are the same. Their size undergoes significant changes compared to PS, leading to the same particles in the range of 50–200 μm. This is due to the removed lignin from PS. Lignin integrates cellulose and hemicellulose, leading to the larger and homogenous PS particles. The similarity of MNC particles to MC proves that the nitration process does not affect on reducing the size and on forming the porosity in MNC.

As shown in Fig. S1D, the PSB particles are observed between 10 and 200 μm, which are smaller than the MC. This confirms that the pyrolysis process causes the destruction and smaller size for the PSB preparation compared to the acid treatment for the MC isolation. Besides, some particles of MC and MNC are seen as smooth and non-porous, while all PSB particles are porous and rough. The porous and irregular structure in PSB was created by the thermal degradation of cellulose, hemicellulose, and lignin molecules in PS. On the other hand, the structural destruction of PS to obtain MC and MNC was also proceeded by acid hydrolysis. Thus, it can be concluded that the destructive effect of thermal degradation on PS was significant compared to the acid degradation.

**Table 3**
Ultimate analysis of CHNSO for PS and PSB based on pre-dehydration, pyrolysis temperature and time. The bold results are the desirable.

| PSB | Pre-dehydration | T (°C) | Time (min) | Product yield (%) | Ultimate analysis (wt%) | | | | | | HHV (MJ/kg) | HHV yield (MJ/kg) |
|---|---|---|---|---|---|---|---|---|---|---|---|---|
| | | | | | C | H | N | S | O | Ash | | |
| 1 | + | 200 | 0 | 67 ± 1.40 | 37.31 ± 0.38 | 3.25 ± 0.04 | 0.44 ± 0.00 | 5.93 ± 0.00 | 49.07 ± 0.32 | 4 | 9.084 ± 0.80 | 6.087 ± 0.12 |
| 2 | | 200 | 30 | 54 ± 1.20 | 51.94 ± 0.50 | 3.09 ± 0.06 | 0.43 ± 0.00 | 1.87 ± 0.00 | 38.67 ± 0.24 | 4 | 15.27 ± 0.14 | 8.245 ± 0.16 |
| 3 | | 300 | 0 | 49 ± 1.00 | 53.89 ± 0.54 | 3.15 ± 0.06 | 0.43 ± 0.00 | 1.69 ± 0.00 | 36.84 ± 0.24 | 4 | 16.323 ± 0.16 | 7.998 ± 0.16 |
| 4 | | 300 | 30 | 38 ± 0.80 | 61.1 ± 0.60 | 2.05 ± 0.04 | 0.57 ± 0.00 | 0 | 32.28 ± 0.22 | 4 | 17.847 ± 0.18 | 6.782 ± 0.16 |
| 5 | | 400 | 0 | 32 ± 0.60 | 65.61 ± 0.64 | 1.87 ± 0.02 | 0.63 ± 0.00 | 0 | 27.89 ± 0.18 | 4 | 19.898 ± 0.20 | 6.347 ± 0.12 |
| **6** | | 400 | 30 | **28** ± 0.60 | 73.1 ± 0.72 | 2.1 ± 0.04 | 0.59 ± 0.00 | 0 | 20.21 ± 0.10 | 4 | **24.124** ± 0.22 | 6.76 ± 0.12 |
| 7 | – | 200 | 0 | 97 ± 2.00 | 48.98 ± 0.50 | 5.93 ± 0.10 | 0.68 ± 0.00 | 0 | 40.41 ± 0.32 | 4 | 17.82 ± 0.18 | 17.356 ± 0.40 |
| 8 | | 200 | 30 | 84 ± 1.60 | 52.66 ± 0.52 | 5.63 ± 0.10 | 0.94 ± 0.00 | 0 | 36.77 ± 0.24 | 4 | 19.285 ± 0.20 | 16.122 ± 0.32 |
| 9 | | 300 | 0 | 33 ± 0.60 | 63.42 ± 0.62 | 2.77 ± 0.04 | 0.87 ± 0.00 | 0 | 28.94 ± 0.12 | 4 | 20.25 ± 0.20 | 6.763 ± 0.12 |
| 10 | | 300 | 30 | 31 ± 0.60 | 64.6 ± 0.64 | 2.63 ± 0.04 | 0.82 ± 0.00 | 0 | 27.95 ± 0.12 | 4 | 20.626 ± 0.20 | 6.435 ± 0.12 |
| 11 | | 400 | 0 | 24 ± 0.40 | 66.5 ± 0.66 | 4.04 ± 0.06 | 1.64 ± 0.00 | 0 | 23.82 ± 0.12 | 4 | 24.008 ± 0.24 | 5.81 ± 0.10 |
| **12** | | 400 | 30 | **24** ± 0.40 | 75.21 ± 0.74 | 3.64 ± 0.04 | 1.42 ± 0.00 | 0 | 15.73 ± 0.10 | 4 | **27.82** ± 0.28 | 6.67 ± 0.12 |
| PS | | – | – | 1 ± 0.00 | 48.98 ± 0.48 | 6.13 ± 0.10 | 0.68 ± 0.00 | 0 | 40.21 ± 0.32 | 4 | 18.14 ± 0.18 | 18.14 ± 0.18 |

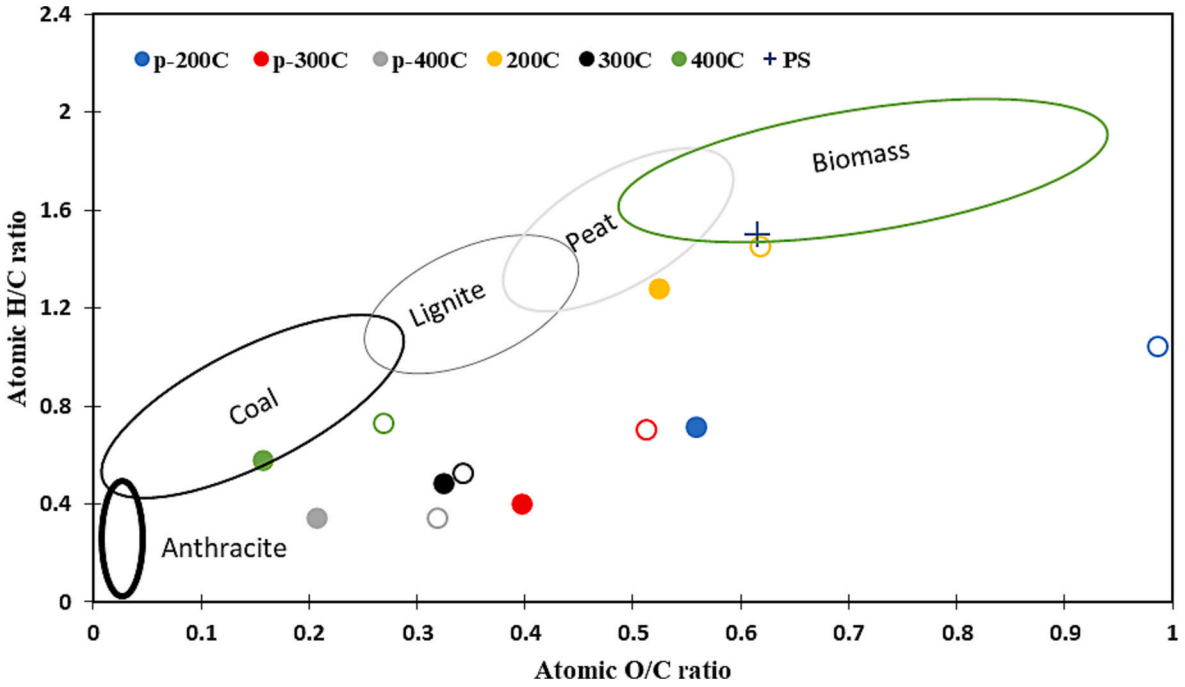


**Fig. 2.** van Krevelen diagram for PS and PSB based on pre-dehydration, pyrolysis temperature and time. Empty circles and p- denote time = 0 min and pre-dehydrated samples, respectively.

**Table 4**
Comparison of various feedstocks and process parameters to produce solid biofuels.

| Feedstock | Pyrolysis temperature (°C) | Pyrolysis time (min) | Pretreatment | Product yield (%) | $HHV_{feedstock}$ (MJ/kg) | $HHV_{biofuel}$ (MJ/kg) | Ref. |
|---|---|---|---|---|---|---|---|
| PS | 400 | 30 | $H_2SO_4$ (98 %) pre-dehydration at room temperature with $H_2SO_4$: raw material = 1.83 (w/w) | 28 ± 0.60 | 18.14 ± 0.18 | 24.12 ± 0.22 | This study |
| PS | 400 | 30 | – | 24 ± 0.40 | 18.14 ± 0.18 | 27.82 ± 0.28 | This study |
| PS | 550 | 30 | – | – | 17.58 | 31.35 | (Jeníček et al., 2023) |
| | 450 | | | – | | 29.71 | |
| | 350 | | | – | | 27.93 | |
| Douglas fir sawdust | 500 | 15 | $H_2SO_4$ (12.5 %) pre-dehydration at 90 °C with $H_2SO_4$: raw material = 1.5 (w/w) | 44 | 19.71 | 31.16 | (Wang et al., 2022) |
| | | | – | 22.4 | | 32.18 | |

### 3.4.2. FTIR analysis

Fig. S2 shows the FTIR spectra of PS, MC, MNC, and PSB. For PS, a broad band in the region of 3400–3500 $cm^{-1}$ is attributed to the stretching vibration of O—H groups. The peak around 2900 $cm^{-1}$ is related to the stretching vibration of C—H alkane bonds. The peak at 1525 $cm^{-1}$ corresponds to aromatic C=C bending in lignin. The peak at 1269 $cm^{-1}$ is ascribed to the C—O—C stretching vibration in hemicellulose, lignin, and cellulose. The peak at 1760 $cm^{-1}$ is assigned to the stretching vibration of C=O bonds in carbonyl, ester, and acetyl groups in xylan and lignin. The C—O—C pyranose ring skeletal vibration is detected at 1065 $cm^{-1}$. Some peaks at 1380–1465 $cm^{-1}$ are associated with the bending vibration of C—H (Kasiri and Fathi, 2018; Movva and Kommineni, 2017).

In MC spectra, the intensity of PS peaks at 2900, 1639, 1380–1465, and 897 $cm^{-1}$ increase because the acid treatment and bleaching remove the lignin and hemicellulose from PS. Lignin masks the main bonds in MC.

In MNC spectra, the symmetric $NO_2$ stretching vibration is detected at 1385 and 1282 $cm^{-1}$. The peak at 1637 $cm^{-1}$ is related to the asymmetric stretching vibration of $NO_2$. The intense peak at around 831 $cm^{-1}$ corresponds to the O–$NO_2$ stretching vibration. Less intense peaks at 754 and 692 $cm^{-1}$ are assigned to the asymmetric and symmetric deformation of O–$NO_2$ groups, respectively. The intensity of MC peak at 3400–3500 $cm^{-1}$ decreases, justifying the nitration of the OH groups (Tarchoun et al., 2019; Trache et al., 2016).

For PSB, it is observed that all peaks for PS disappear except the peaks at 3400–3500, 1707, and 1612 $cm^{-1}$. They are observed less intense peaks than those in PS spectra because the OH, COOH, and C=O groups are removed from the structure of PS under the pyrolysis process (Barskov et al., 2019).

### 3.4.3. XRD

Fig. S3 illustrates the XRD patterns of PS, MC, MNC, and PSB. For PS, the peaks around 2θ = 16.5°, 22°, and 35° indicate crystalline regions attributed to the cellulose structure of PS (Marett et al., 2017). For MC, the peaks at 2θ = 15.5°, 22.4°, 31.9°, and 35° demonstrate the crystalline cellulose with the CrI = 86 %. Compared to PS, MC crystallinity is enhanced because nitric acid dissolves hemicellulose and lignin, as well as most of the amorphous structures of PS, leading to a narrower and more intensive crystalline peak. Compared to other studies reporting the crystallinities of PS cellulose from 67 to 85 %, this is a remarkable result (Kasiri and Fathi, 2018; Marett et al., 2017; Robles et al., 2021).

For MNC, the peak at 2θ = 22.6° results in the crystalline nitrocellulose with the CrI = 79 %. The accessibility of OH groups can provide some intramolecular and intermolecular hydrogen bonds, leading to the ordered crystalline arrangements. Compared to MC, MNC crystallinity is

reduced because of the substitution of OH groups by O–$NO_2$ (Trache et al., 2016). Compared to other research obtaining MNC with a crystallinity from 22.6 to 66.2 %, this study archives a higher crystallinity (Meng et al., 2020; Tarchoun et al., 2019; Trache et al., 2016). Therefore, according to the characterizations, pure microcrystalline cellulose and microcrystalline nitrocellulose were obtained by nitric acid extraction.

As seen in the XRD pattern of PSB, no peaks are detected to prove its crystallinity. Thus, PSB was obtained as an amorphous solid biofuel because the thermal degradation (pyrolysis) decomposed the cellulose structure of PS, destroying its crystalline regions.

### 3.4.4. Thermal analysis

Fig. S4 depicts the TGA and DTG curves of PS, MC, MNC, and PSB. The PS curve demonstrates its thermal decomposition in three stages. The first stage indicates the evaporation of water from 50 to around 120 °C. The second stage displays the most weight loss (55 %) due to the decomposition of cellulose and hemicellulose from 250 to 370 °C. The third stage shows a 35 % mass loss due to the destruction of lignin and carbonic residues from 370 °C to the end. The small shoulder (bump) indicates the primary decomposition of hemicellulose, lignin, and other non-cellulosic components (Kasiri and Fathi, 2018; Peters, 2011).

Similar to PS, the first stage of MC decomposition corresponds to the water evaporation from 50 to around 120 °C. After that, the most mass loss (55 %) occurs from 250 to 340 °C with a single intense exothermic decomposition process. The final mass loss (32 %) is detected from 340 to 525 °C.

The thermal decomposition of MNC occurs in three stages. The onset temperature of the thermal decomposition of MNC is 60 °C. Two intense exothermic peaks for MNC, detected by the DTG curve, prove the decomposition process at 60–140 °C and 140–250 °C with a mass loss of 20 and 40 %, respectively. Compared with MC, the thermal stability of MNC decreases slightly because of increasing its nitrogen content (Meng et al., 2020). The final stage of MNC decomposition shows a 40 % mass loss from 250 to 560 °C.

The PSB curve exhibits its thermal decomposition in two stages. The first stage corresponds to water evaporation in the range of 50–140 °C. The final stage, from 140 to 600 °C, shows the most mass loss (75 %) due to the decomposition of cellulose, hemicellulose, lignin, and carbonized structures that remain in PSB after the pyrolysis of PS at 400 °C for 30 min.

## 3.5. Economic assessment

The cost analysis of the production of MC, MNC, and PSB from PS is given in Table 5. Positive NPV for MNC production proposes that the efficient investment in the scenario simulated will be feasible during the real-time implementation. The NPV is estimated at 25 % and 7 % interest for the production in Iran and others, respectively. Economic assessment of NC production from palm oil empty fruit bunches via ammonium hydroxide and sulfuric acid pretreatment demonstrates that its production is profitable because ROI, payback period, NPV, and IRR are 11.49 %, 5.85 years, 442,427 $, and 13.35 % (Panjaitan and Gozan, 2021). However, they are far from the values obtained for the MNC production in this work. Therefore, this study proposes the most profitable production of MNC compared to the literature.

Although NPV for MC is calculated as negative, its ROI, IRR, and payback period indicate the feasible investment in its project. Economic analysis of cellulose production from rice husk by chlorine extraction shows a positive NPV with a payback period of 0.42 years and ROI of 240.64 %, which makes it more feasible compared to the MC production in this research (Hafid et al., 2021). Techno-economic analysis assessment of cellulose nanocrystal production from wood pulp results in a positive NPV, a payback period of 3.94 years, ROI of 25.38 %, and IRR of 30.40 %, which proves the MC production from PS can be a fast economic plan compared to it (Rajendran et al., 2023). Techno-economic analysis of MC production from pulp exhibits ROI of 69.2 % and a net profit of 17.3 €/kg (Vanhatalo et al., 2014). Compared to the literature focusing on the production of cellulose and its economics, this study suggests the first feasible production of MC from agricultural residues.

According to the net profit, the PSB production is not profitable, and it cannot compete with coal because coal is daily produced and its reservoirs are scattered all over the world, reducing its price. However, it is not a renewable resource. Consequently, the PSB production will be economically justified by reducing coal reserves and increasing its price over time. In agreement with this study, economic analysis of biochars derived from different feedstocks shows ROI of 17.59 %, a payback period of 8.3–20 years, and IRR of 7.8–8.96 %, which does not attract producers to invest (Haeldermans et al., 2020; Mishra et al., 2023; Zhang et al., 2021).

It is noted that each government's policies for bank interest rates, taxes, and annual inflation can affect the economic parameters, changing the profitability analysis. In Iran, inflation and bank interest rates are highly sensitive to political conditions. The difference between the annual inflation and the bank interest rate can increase the production profit. Thus, the countries whose annual inflation is far from their

**Table 5**
The cost analysis of the production of MC, MNC, and PSB from PS.

| Item | Amount | | |
|---|---|---|---|
| | MC | MNC | PSB |
| Equipment & installation costs (A) | | | |
| Grinder | 11,850 $ | 11,850 $ | 11,850 $ |
| Sieve | 9000 $ | 9000 $ | 9000 $ |
| Mixing tank (furnace) | 79 $ | 119 $ | 4600 $ |
| Dryer | 15,893 $ | 19,867 $ | 0 |
| Capital costs (B) | | | |
| Land, building & construction | 93,000 $ | 93,000 $ | 93,000 $ |
| Material costs (C) | | | |
| PS | 367 $/yr | 367 $/yr | 65,456 $/yr |
| $HNO_3$ | 38,708 $/yr | 40,403 $/yr | 0 |
| $H_2SO_4$ | 0 | 65 $/yr | 0 |
| NaClO | 10,831 $/yr | 10,831 $/yr | 0 |
| Utility costs (D) | | | |
| Water | 47,180 $/yr | 53,263 $/yr | 0 |
| Electricity | 26,390 $/yr | 30,952 $/yr | 6912 $/yr |
| Labor costs (E) | | | |
| Operating labor | 12,000 $/yr | 12,000 $/yr | 12,000 $/yr |
| Maintenance labor | 1200 $/yr | 1200 $/yr | 1200 $/yr |
| Supervisor | 3600 $/yr | 3600 $/yr | 3600 $/yr |
| Supplies costs (F) | | | |
| Operating supplies | 4000 $/yr | 4000 $/yr | 4000 $/yr |
| Fixing & maintenance costs (G) | | | |
| Equipment fixing | 820 $/yr | 910 $/yr | 570 $/yr |
| General works costs (H) | | | |
| General & administratives | 24,000 $/yr | 24,000 $/yr | 24,000 $/yr |
| Property insurance & tax | 85,453 $/yr | 4,157,498 $/yr | 23,664 $/yr |
| Total capital investment (A + B) | 129,823 $ | 133,835 $ | 118,450 $ |
| Total annual operating cost (I = C + D + E + F + G + H) | 244,547 $/yr | 4,339,086 $/yr | 141,398 $/yr |
| Annual production (J) | 6781 kg/yr | 8477 kg/yr | 720,000 kg/yr |
| Net production cost (K = I / J) | 37.54 $/kg | 511.9 $/kg | 0.2 $/kg |
| Net production revenue (L) | 60 $/kg | 2450 $/kg | 0.14 $/kg |
| Net profit (M = L − K) | 22.46 $/kg | 1938 $/kg | −0.06 $/kg |
| Net profit margin (M / L) | 37.44 % | 79.11 % | −44.4 % |
| ROI (M * J / (A + B)) | 117.33 % | 12,274.82 % | – |
| Payback time ((A + B) / (M * J)) | 0.85 yr | 0.01 yr | – |
| IRR | 117 % | 12,275 % | – |
| NPV at 25 % interest | −4759 $ | 20,127 $ | – |
| NPV at 7 % interest | −13,508 $ | 276,628 $ | – |

interest rate make an economic opportunity to produce products cost-effectively. On the other hand, the value of the national currency decreases in Iran every year. Further, due to Iran's government subsidies, the price of energy and water, and the income taxes for industries are much lower compared to other countries. Therefore, the investment in MC and MNC production, and in other productions are cost-effective in Iran.

## 4. Conclusions

This study showed that the production of MC and MNC from PS was economically feasible. Microcrystalline cellulose particles with 100 % purity were achieved for the first time via a rapid recyclable nitric acid treatment in one stage, which was superior to the alkaline-extracted cellulose. The valorization of PS as a feedstock of nitrocellulose resulted in the MNC particles with a nitrogen content of 10.81 %, obtained from the MC using a facile synthesis economically competitive with other methods. The incorporation of sulfuric acid pre-dehydration with pyrolysis temperature and time improved the product yield of PSB, but lowering the HHV values.

## CRediT authorship contribution statement

**Alireza Chackoshian Khorasani:** Conceptualization, Supervision, Project administration, Validation, Writing – review & editing. **Saeed Zeinabadi Bajestani:** Investigation, Formal analysis, Methodology. **Alireza Saadat Bajestani:** Resources, Writing – original draft.

## Declaration of competing interest

The authors declare the following financial interests/personal relationships which may be considered as potential competing interests: Alireza Chackoshian Khorasani reports financial support was provided by Ferdowsi University of Mashhad.

## Data availability

Data will be made available on request.

## Acknowledgements

The authors gratefully acknowledge the financial support (Grant No. 1/58955) provided by Ferdowsi University of Mashhad. This study was also supported by Iran National Science Foundation (INSF) (Grant No. 4002262).

## Appendix A. Supplementary data

Supplementary data to this article can be found online at https://doi.org/10.1016/j.biteb.2023.101673.

## References

Açıkalın, K., 2012. Pyrolytic characteristics and kinetics of pistachio shell by thermogravimetric analysis. J. Therm. Anal. Calorim. 109, 227–235.
Barskov, S., Zappi, M., Buchireddy, P., Dufreche, S., Guillory, J., Gang, D., Hernandez, R., Bajpai, R., Baudier, J., Cooper, R., 2019. Torrefaction of biomass: a review of production methods for biocoal from cultured and waste lignocellulosic feedstocks. Renew. Energy 142, 624–642.
Boufi, S., Chaker, A., 2016. Easy production of cellulose nanofibrils from corn stalk by a conventional high speed blender. Ind. Crop. Prod. 93, 39–47.
Cheng, M., Qin, Z., Hu, J., Liu, Q., Wei, T., Li, W., Ling, Y., Liu, B., 2020. Facile and rapid one–step extraction of carboxylated cellulose nanocrystals by $H_2SO_4/HNO_3$ mixed acid hydrolysis. Carbohydr. Polym. 231, 115701.
Gismatulina, Y.A., Budaeva, V.V., Sakovich, G.V., 2018. Nitrocellulose synthesis from miscanthus cellulose. Propellants Explos. Pyrotech. 43, 96–100.
Gupta, S., Gupta, G.K., Mondal, M.K., 2022. Thermal degradation characteristics, kinetics, thermodynamic, and reaction mechanism analysis of pistachio shell pyrolysis for its bioenergy potential. Biomass Convers. Biorefin. 12, 4847–4861.
Haeldermans, T., Campion, L., Kuppens, T., Vanreppelen, K., Cuypers, A., Schreurs, S., 2020. A comparative techno-economic assessment of biochar production from different residue streams using conventional and microwave pyrolysis. Bioresour. Technol. 318, 124083.
Hafid, H.S., Omar, F.N., Zhu, J., Wakisaka, M., 2021. Enhanced crystallinity and thermal properties of cellulose from rice husk using acid hydrolysis treatment. Carbohydr. Polym. 260, 117789.
Jeníček, L., Tunklová, B., Malaťák, J., Velebil, J., Malaťáková, J., Neškudla, M., Hnilička, F., 2023. The impact of nutshell biochar on the environment as an alternative fuel or as a soil amendment. Materials (Basel) 16, 2074.
Kasiri, N., Fathi, M., 2018. Production of cellulose nanocrystals from pistachio shells and their application for stabilizing Pickering emulsions. Int. J. Biol. Macromol. 106, 1023–1031.
Lipin, V.A., Petrova, I.I., Sofronova, E.D., 2020. Alternative feedstock for producing nitrocellulose. Fibre Chem. 52, 201–204.
Marett, J., Aning, A., Foster, E.J., 2017. The isolation of cellulose nanocrystals from pistachio shells via acid hydrolysis. Ind. Crop. Prod. 109, 869–874.
Meng, X., Pu, C., Cui, P., Xiao, Z., 2020. Preparation, thermal and sensitivity properties of nano-sized spherical nitrocellulose composite crystal. Propellants Explos. Pyrotech. 45, 1194–1203.
Mishra, R.K., Kumar, D.J.P., Narula, A., Chistie, S.M., Naik, S.U., 2023. Production and beneficial impact of biochar for environmental application: a review on types of feedstocks, chemical compositions, operating parameters, techno-economic study, and life cycle assessment. Fuel 343, 127968.
Movva, M., Kommineni, R., 2017. Extraction of cellulose from pistachio shell and physical and mechanical characterisation of cellulose-based nanocomposites. Mater. Res. Express 4, 45014.
Muvhiiwa, R., Mawere, E., Moyo, L.B., Tshuma, L., 2021. Utilization of cellulose in tobacco (*Nicotiana tobacum*) stalks for nitrocellulose production. Heliyon 7.
Özbek, H.N., Yanık, D.K., Fadıloğlu, S., Göğüş, F., 2020. Ultrasound-assisted alkaline pre-treatment and its sequential combination with microwave for fractionation of pistachio shell. Renew. Energy 157, 637–646.
Özbek, H.N., Koçak Yanık, D., Fadıloğlu, S., Göğüş, F., 2021. Effect of microwave-assisted alkali pre-treatment on fractionation of pistachio shell and enzymatic hydrolysis of cellulose-rich residues. J. Chem. Technol. Biotechnol. 96, 521–531.
Paloheimo, L., Kero, M.-L., 1962. A method for cellulose determination. Agric. Food Sci. 34, 57–65.
Panjaitan, J.R.H., Gozan, M., 2021. Techno-economic evaluation of nitrocellulose production from palm oil empty fruit bunches. ASEAN Eng. J. 11, 246–254.
Pattnaik, F., Nanda, S., Kumar, V., Naik, S., Dalai, A.K., 2022. Isolation of cellulose fibers from wetland reed grass through an integrated subcritical water hydrolysis-pulping-bleaching process. Fuel 311, 122618.
Peters, B., 2011. Prediction of pyrolysis of pistachio shells based on its components hemicellulose, cellulose and lignin. Fuel Process. Technol. 92, 1993–1998.
Rajendran, N., Runge, T., Bergman, R.D., Nepal, P., Houtman, C., 2023. Techno-economic analysis and life cycle assessment of cellulose nanocrystals production from wood pulp. Bioresour. Technol. 377, 128955.
Robles, E., Izaguirre, N., Martin, A., Moschou, D., Labidi, J., 2021. Assessment of bleached and unbleached nanofibers from pistachio shells for nanopaper making. Molecules 26, 1371.
Saginovich, I.Y., Ayazbayuly, M.N., Mustafinovich, S.K., 2020. Production of nitrocellulose from cellulose cultivated in South Kazakhstan under supercritical conditions. In: Известия НАН РК. Серия хиМии и технологии, pp. 30–35.
Santos, D., Iop, G.D., Bizzi, C.A., Mello, P.A., Mesko, M.F., Balbinot, F.P., Flores, E.M.M., 2021. A single step ultrasound-assisted nitrocellulose synthesis from microcrystalline cellulose. Ultrason. Sonochem. 72, 105453.
Tarchoun, A.F., Trache, D., Klapötke, T.M., Chelouche, S., Derradji, M., Bessa, W., Mezroua, A., 2019. A promising energetic polymer from Posidonia oceanica brown algae: synthesis, characterization, and kinetic modeling. Macromol. Chem. Phys. 220, 1900358.
Trache, D., Donnot, A., Khimeche, K., Benelmir, R., Brosse, N., 2014. Physico-chemical properties and thermal stability of microcrystalline cellulose isolated from Alfa fibres. Carbohydr. Polym. 104, 223–230.
Trache, D., Khimeche, K., Mezroua, A., Benziane, M., 2016. Physicochemical properties of microcrystalline nitrocellulose from Alfa grass fibres and its thermal stability. J. Therm. Anal. Calorim. 124, 1485–1496.
Vanhatalo, K.M., Parviainen, K.E., Dahl, O.P., 2014. Techno-economic analysis of simplified microcrystalline cellulose process. BioResources 9, 4741–4755.
Wang, C., Zou, R., Qian, M., Kong, X., Huo, E., Lin, X., Wang, L., Zhang, X., Ruan, R., Lei, H., 2022. Improvement of the carbon yield from biomass carbonization through sulfuric acid pre-dehydration at room temperature. Bioresour. Technol. 355, 127251.
Wang, J., Li, X., Song, J., Wu, K., Xue, Y., Wu, Y., Wang, S., 2020. Direct preparation of cellulose nanofibers from bamboo by nitric acid and hydrogen peroxide enables fibrillation via a cooperative mechanism. Nanomaterials 10, 943.
Zhang, Z., Delcroix, B., Rezazgui, O., Mangin, P., 2021. Simulation and techno-economic assessment of bio-methanol production from pine biomass, biochar and pyrolysis oil. Sustain. Energy Technol. Assess. 44, 101002.